Available online at www.sciencedirect.com

SciVerse ScienceDirect

Ceramics International 39 (2013) 1081–1086

CERAMICS INTERNATIONAL

www.elsevier.com/locate/ceramint

Rutile TiO_2(101) based plasmonic nanostructures

S. Sankar[a,b], K.G. Gopchandran[a,*]

[a]Department of Optoelectronics, University of Kerala, Kariavattom, Trivandrum 695 581, India
[b]Department of Physics, Sree Narayana College, Punalur, Kerala, India

Received 24 April 2012; received in revised form 6 July 2012; accepted 6 July 2012
Available online 17 July 2012

Abstract

TiO_2/Ag and TiO_2/Au nanocrystalline multilayer thin films were deposited using pulsed laser deposition technique. Investigations have been made to understand the influence of different phases of TiO_2 on the surface plasmon characteristics of the thin films. Rutile phase of TiO_2 is found to be a good host matrix for both Ag and Au nanoparticles. Compared to silver, gold nanoparticles are found to enhance the photocatalytic activity of the films by exhibiting a broad and intense absorption with a significant shift to longer wavelength region.

Keywords: B. Nanocomposites; B. Surface; D. TiO_2; Surface plasmon resonance

1. Introduction

Optical properties of noble metal nanoparticles such as gold and silver have been extensively studied by many researchers [1,2]. The intense resonances in the optical spectra of these particles are due to the collective oscillation of conduction band electrons, known as a localized surface plasmon [3]. Organic frameworks [4] and metal oxide supports [5] have frequently been used to maintain the dispersion of such noble metal nanoparticles. TiO_2 is an active support for promoting the catalytic performance of Ag or Au [6]. TiO_2 is a typical semiconductor having high corrosion resistance, chemical stability and optical transparency in the visible and near infrared regions and high refractive index. The combination of semiconductor substrate and metal cluster showed improved photocatalytic activity by trapping the photo-induced charge carriers, thereby improving the charge transfer processes [7].

To make the use of noble metals more economically and to improve their performance, it is crucial to control both the size of nanoparticles and their dispersity on the support. Titanium based nanostructures can be suitably designed to yield enhanced optical and catalytic properties, utilizing the possibility of photo excitation of the electron from the TiO_2 shell to the metal core [8]. Ag can serve as electron trap aiding electron-hole separation, and can also facilitate electron excitation by creating a local electric field [9]. The higher activity was attributed to the trapping of the conduction band electrons by Ag nanoparticles, which prevents the electron-hole recombination, thereby enhancing the redox reactions on the TiO_2 surface. Extensive research is being done on the optical activity, reflectivity properties, photo-sensitization and thermal stability of TiO_2/Au films. Despite the chemical inertness of bulk gold, Au nanoparticles (NPs) supported on metal oxide surfaces show surprisingly high chemical activity [10]. The optical properties of these multilayer structures are dominated in the visible region by the surface plasmon resonance (SPR) of the noble metal nanoparticles [11]. In this work, TiO_2/Ag and TiO_2/Au multilayer nanostructures exhibiting surface plasmon resonance are prepared using pulsed laser deposition technique. Influence of phase, crystallinity and morphology of TiO_2 surfaces on the plasmon resonance characteristics of Ag and Au nanoparticles are investigated in detail.

2. Experimental

TiO_2 thin film matrixes were prepared using pulsed laser deposition technique by employing a Q- switched Nd: YAG

---

*Corresponding author.
E-mail address: gopchandran@yahoo.com (K.G. Gopchandran).

0272-8842/$36.00 © 2012 Elsevier Ltd and Techna Group S.r.l. All rights reserved.
http://dx.doi.org/10.1016/j.ceramint.2012.07.030

laser (Quanta-Ray INDI-series, Spectra Physics) source with 150 mJ of laser energy at 532 nm, pulse width 8 ns and repetition frequency 10 Hz. TiO_2 powder (99.99% pure, from Sigma Aldrich Company), thoroughly grinded in an agate mortar and pressed into the form of a pellet in a hydraulic press and sintered at 1000 °C for 4 h, was used as the target material for the ablation process in the preparation of the host matrix. Fused amorphous quartz plates were used as substrates. Before starting the ablation process, the base pressure in the deposition chamber was brought down to $\sim 10^{-8}$ Pa. Pure oxygen was circulated in the evacuated chamber through a gas inlet valve and the oxygen pressure within the chamber was maintained at 1×10^{-4} Pa during the deposition. Duration of the deposition was of 45 min. The films were deposited at a substrate temperature of 30 °C. The as deposited amorphous films were subjected to annealing at different temperatures viz. 500, 700 and 1000 °C to obtain anatase, anatase-rutile and rutile phases of TiO_2, respectively. Ag and Au nanoparticles were deposited in to these TiO_2 host matrixes using laser energy of 20 mJ for 10 min using 99.99% pure Ag and Au pellets as targets under a vacuum of $\sim 10^{-8}$ Pa. The structure and crystallinity of the films were analyzed by grazing incidence X-ray diffraction (GIXRD) using Siemens D5000 diffractometer. The surface morphologies of the films were investigated using scanning electron microscopy (SEM) technique using the system Siron. Compositional studies were done using EDS and XPS. The X-ray photoelectron spectroscopy (XPS) data were recorded with the specimen mounted on a specially designed sample holder using an AlKα laboratory X-ray source [12]. The data were recorded with 20 eV pass energy with 1 eV energy resolution. The chamber base pressure was 6×10^{-13} Pa. Optical measurements were conducted in the wavelength range 300–900 nm using a double beam UV–visible spectrophotometer, Jasco-V 550. Thickness of the films was measured using Dektak 6M bench-top surface profiler and is found to be in the range from 250 to 300 nm.

3. Results and discussions

3.1. GIXRD, XPS and EDX studies

The X-ray diffraction pattern of the rutile TiO_2 host matrixes used for depositing Ag and Au metal nanoparticles as shown in Fig. 1(a)–(c) shows the X-ray diffraction patterns of rutile TiO_2 matrixes deposited with Au and Ag nanoparticles. All the peaks in these XRD patterns are indexed according to JCPDS file 21-1276 corresponding to rutile phase of TiO_2. No XRD peak corresponding to Ag or Au can be seen in these patterns, which can be attributed either to the well dispersed distribution of these nanoparticles or to the lack of crystallization of these particles in the TiO_2 host matrix [13,14].

Investigations made with X-ray photoelectron spectroscopy clearly showed the presence of both Au and Ag on the film surface. In Fig. 2(a), the oxidation and spin state of the Ti atoms corresponding to $Ti2p_{1/2}$ and $Ti2p_{3/2}$ peaks, indicate the presence of Ti^{4+} ions in the host matrix. Presence of O^{2-} ions in host matrix is evident from O1s peak shown in Fig. 2(b). Ti2p and O1s peaks of TiO_2 are observed around at binding energies of 458 and 530 eV. XPS spectra of rutile TiO_2/Ag and rutile TiO_2/Au multilayer thin films are shown in Figs. 3 and 4 respectively. Based on XPS results, the surface elemental compositions of TiO_2/Ag and TiO_2/Au thin films are determined. A comparison of the locations of the binding

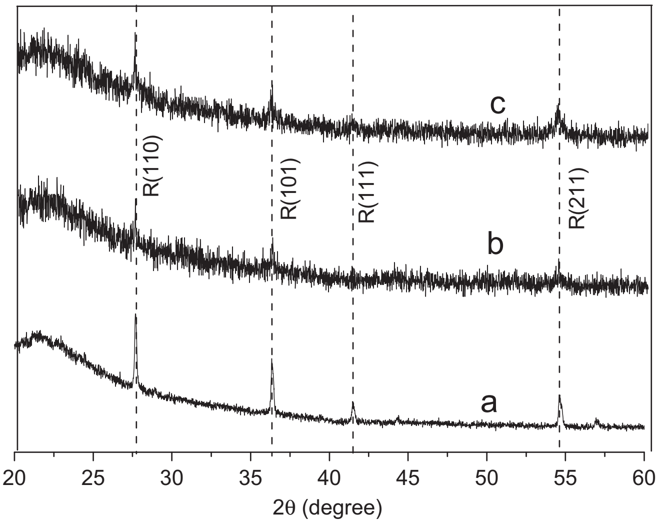

Fig. 1. GIXRD patterns of (a) rutle TiO_2 matrix; multilayer thin films of (b) TiO_2/Ag. and (c) TiO_2/Au.

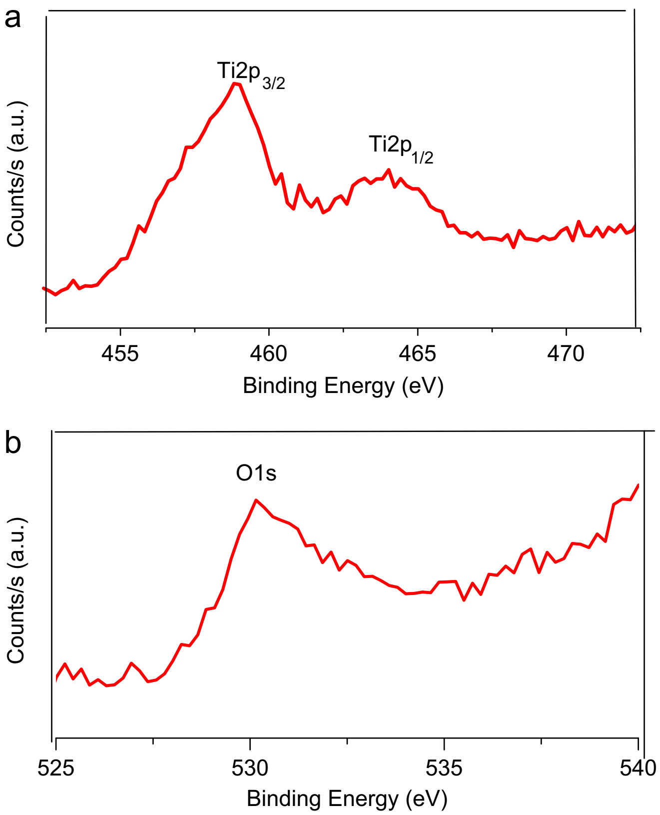

Fig. 2. XPS spectrum of rutile TiO_2 substrate with photoelectron peaks corresponding. to (a) Ti2p and (b) O1s.

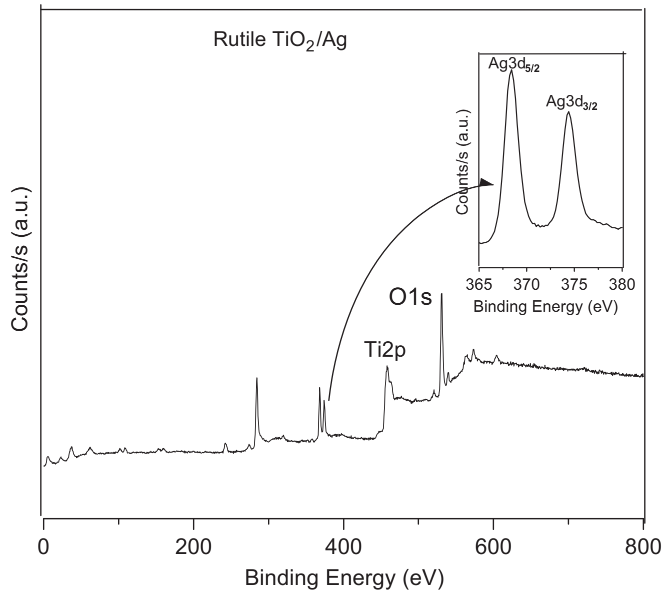

Fig. 3. Wide XPS spectrum of Rutile (101) TiO$_2$/Ag thin film. Inset: XPS. spectrum of Ag nanoparticles deposited on Rutile (101) TiO$_2$ matrix.

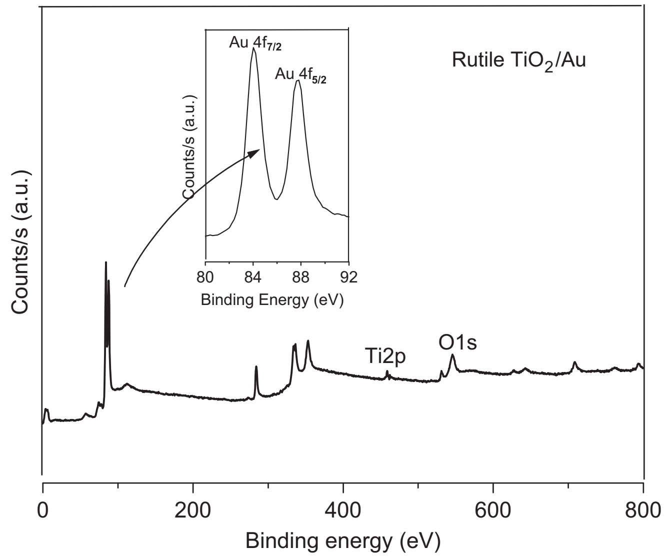

Fig. 4. Wide XPS spectrum of Rutile (101) TiO$_2$/Au thin film. Inset: XPS. spectrum of Au nanoparticles deposited on Rutile (101) TiO$_2$ matrix.

energies of photoelectron peaks corresponding to rutile TiO$_2$/Ag and TiO$_2$/Au obtained in this investigation with that of the other reported values given in Table 1.

The XPS spectra of silver nanoparticles in rutile TiO$_2$ matrixes are observed at 367 eV and are shown in the inset of Fig. 3. The Ag3d region of the XPS spectrum consists of two main peaks corresponding Ag3d$_{5/2}$ and Ag3d$_{3/2}$ doublet. The surface elemental studies of TiO$_2$/Au multilayer thin films using XPS, shown in Fig. 4 clearly indicated the existence of Au on the surface. In the wide spectrum, Au4f peak appears quite strong because of its higher photo ionization cross-section compared to that of the host matrix. Fitting procedure result for Au4f region is presented in the inset of Fig. 4. The Au4f region of the XPS spectrum consists of two main peaks corresponding to Au4f$_{7/2}$ and Au4f$_{5/2}$ doublet with peak positions at 83 and 87 eV respectively.

Table 1
XPS binding energies of TiO$_2$/Ag and TiO$_2$/Au multilayers.

Material	Species	Binding energy (eV)	Reference
TiO$_2$	Ti^{4+}	459.18 (Ti2p$_{3/2}$)	This work
		458.10 (Ti2p$_{3/2}$)	[15]
		459.4 (Ti2p$_{3/2}$)	[16]
		459.1 (Ti2p$_{3/2}$)	[17]
		464.69 (Ti2p$_{1/2}$)	This work
		463.70 (Ti2p$_{1/2}$)	[15]
	O$_2^-$	531.75(O1s)	This work
		531(O1s)	[17]
		531.30 (O1s)	[15]
Ag	Ag	368.38 (Ag3d$_{3/2}$)	This work
		374.40 (Ag3d$_{3/2}$)	This work
		368.10 (Ag3d$_{5/2}$)	[19]
		373.52 (Ag3d$_{3/2}$)	[19]
	Au	84.02 (Au4f$_{7/2}$)	This work
		87.71(Au4f$_{5/2}$)	This work
		84.00 (Au4f$_{7/2}$)	[18]
		87.70 (Au4f$_{5/2}$)	[18]

Elemental analysis of TiO$_2$/Ag and TiO$_2$/Au thin films were done using energy dispersive spectroscopy (EDX). The results of the EDX spectroscopy analysis indicated the presence of elements Ti, O, Si and Ag/Au on the thin film samples.

3.2. SEM studies

Fig. 5 shows the SEM images of rutile TiO$_2$/Ag and rutile TiO$_2$/Au multilayer thin films. Analysis of these images was done considering the fact that heavier elements (Au and Ag) backscatter electrons more strongly than lighter elements (Ti and O). Silver nanoparticles are found to be homogenously dispersed in the TiO$_2$ matrix and the image shows limited aggregation of Ag nanoparticles inside the matrix. From the images, it can be seen that the rutile TiO$_2$ host matrixes consist of well crystallized large grains. Comparing the morphology of TiO$_2$/Ag and TiO$_2$/Au composite films, Ag nanoparticles are found to be uniformly distributed all over the surface while Au nanoparticles are found to be dispersed in the interfacial regions between adjacent TiO$_2$ grains. At the interface between two TiO$_2$ grains, the Au nanoparticles are found to be aligned along the boundary. This can be attributed to strong interactions including van der Waals forces in between these nanoparticles and adjacent TiO$_2$ crystallites [20]. Au atom–oxygen vacancy complexes can be formed on the surfaces during deposition. The metal atom diffusion length at room temperature, corresponding to Au nanoparticles, is sufficient for preferential nucleation at relatively strong bound sites present at the grain boundaries. The observed alignment of Au nanoparticles along the grain boundaries may be due to the diffusion of the

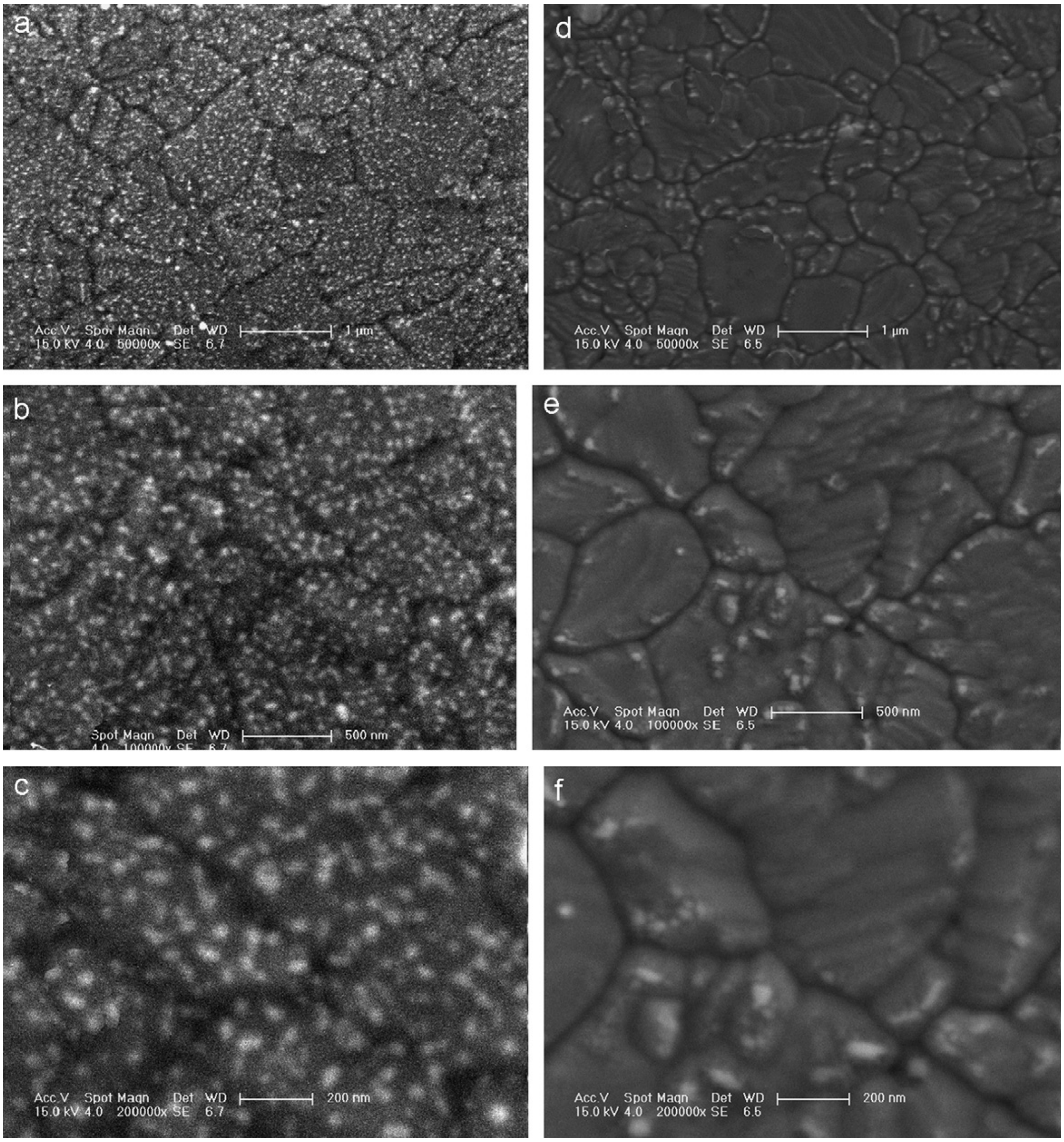

Fig. 5. SEM images under different magnifications: (a), (b) and (c) rutile. TiO_2/Ag; (d), (e) and (f) rutile TiO_2/Au thin films.

atom-vacancy complexes to these regions. The homogeneous dispersion of Ag nanoparticles can be attributed to a self-limiting growth mechanism exhibited by it during deposition [21,22]. The less number of Au nanoparticles compared to that of Ag in TiO_2 surfaces can be attributed to the difference in magnitude of spatial expansion of the plasma of Au and Ag in the laser ablation processes including the interaction and chemical reaction within the plasma as it depends of energy requirements, which is high for gold.

3.3. Optical properties

The optical absorption spectra corresponding to TiO_2 host matrixes are shown in Fig. 6. The optical absorption spectra of multilayer thin films with Ag and Au deposited on TiO_2 surfaces having different crystalline phases are shown in Figs. 7 and 8 respectively. From Fig. 7, it can be seen that Ag nanoparticles deposited on rutile (101) TiO_2 matrix shows maximum absorption at 498 nm.

Silver and gold nanoparticles with size smaller than the wavelength of light exhibit a strong absorption band, due to the surface plasmon resonance in the metal [23]. Also, theoretical approaches, such as the Maxwell–Garnett model [24], predict that the SPR is situated in the visible region of the light spectra in the case of noble metals dispersed in oxide materials. Silver nanoparticles deposited on TiO_2 matrix extend the absorption range of TiO_2 films to the visible region. Therefore, silver nanoparticles promote significantly the photocatalytic activity of TiO_2. Similarly the broad surface plasmon absorption observed in the TiO_2/Au thin films indicates the enhanced photocatalytic activity. The reduction of the size and dimensionality of metals results in a drastic change in the electronic properties as the spatial length scale of the electronic motion is reduced

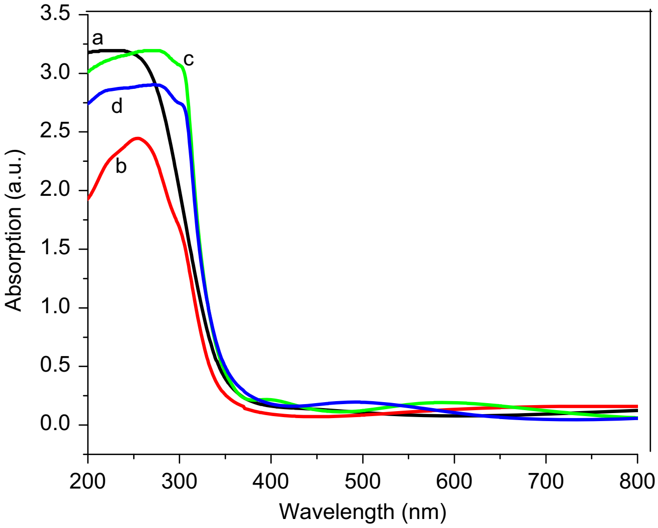

Fig. 6. Absorption spectra of (a) amorphous TiO_2, (b) anatase TiO_2, (c) anatase-rutile TiO_2 and (d) rutile TiO_2 thin films.

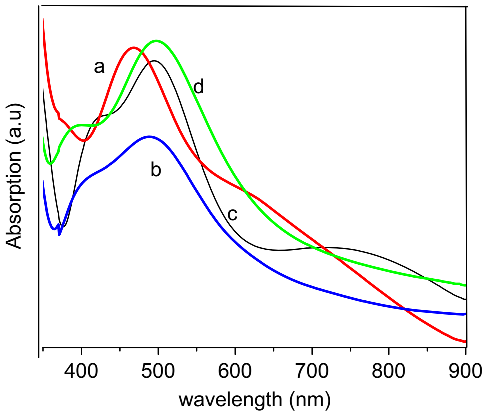

Fig. 7. Absorption spectra of thin films of (a) amorphous TiO_2/Ag, (b) anatase TiO_2/Ag, (c) anatase-rutile TiO_2/Ag and (d) rutile TiO_2/Ag.

[25,26]. Gold nanoparticles absorb and scatter light in orders of magnitudes higher than that of other materials. The physical origin of the strong light absorption by noble metal nanoparticles is the coherent oscillation of the conduction band electrons induced by interaction with an electromagnetic field. It has been shown that SPR can be controlled by particle–particle interaction dictated by interparticle distance and the particle volume [27–29].

Plasmon resonance in the TiO_2/Ag and TiO_2/Au multilayer thin films strongly depends on the crystalline phase, dielectric constant and the surface morphology of the host matrix. The resonance wavelength of the surface plasmon in metal nanoparticles is largely dependent on the environment around the particles. Positions of SPR absorption peaks corresponding to silver and gold nanoparticles obtained are given in Table 2 and the observed redshift of the SPR band can be attributed to the modification of the optical properties of the matrix [30]. TiO_2 matrix of rutile (101) surface has the high refractive index compared to other phases and hence can contribute to an increase in dielectric environment to the metal nanoparticles deposited on it. The observed red shift in the SPR spectrum can be attributed to this fact.

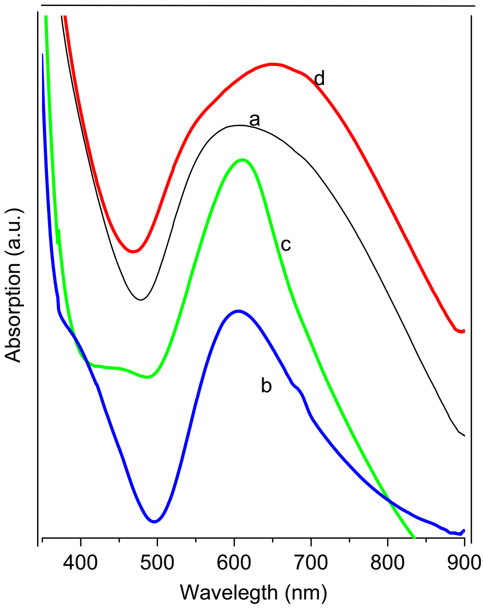

Fig. 8. Absorption spectra of thin films of (a) amorphous TiO_2/Au, (b) anatase. TiO_2/Au, (c) anatase-rutile TiO_2/Au and (d) rutile TiO_2/Au.

Table 2
SPR peak positions in TiO_2/Ag and TiO_2/Au multilayer thin films.

Phase of TiO_2 host matrix	SPR peak (nm)	
	Ag	Au
Amorphous	466	600
Anatase	487	603
Anatase-rutile mixed	494	610
Rutile	498	641

4. Conclusions

TiO_2 (101)/Ag and Au nanocrystalline multilayered thin films exhibiting surface plasmon resonance were synthesized using the pulsed laser deposition technique. Influence of different phases of TiO_2 substrate on the plasmonic characteristics of Ag and Au nanoparticles is studied. Rutile TiO_2 surface is found to be an excellent host matrix for both Ag and Au nanoparticles. Both silver and gold nanoparticles are found to enhance the photocatalytic activity of the TiO_2 thin films by showing a broad and intense absorption band with a significant shift to longer wavelength region.

Acknowledgments

The XPS work was performed at UGC-DAE Consortium for Scientific Research, Indore. A. Rai and S.R. Barman are thanked for their support.

References

[1] A.L. Gonzalez, J.A. Reyes-Esqueda, C. Noguez, Optical properties of elongated noble metal nanoparticles, Journal of Physical Chemistry C 112 (2008) 7356–7362.

[2] S.L. Smitha, K.G. Gopchandran, T.R. Ravindran, V.S. Prasad, Gold nanorods with finely tunable longitudinal surface plasmon resonance as SERS substrates, Nanotechnology 22 (2011) 265705 1-7.

[3] W.L. Barnes, A. Dereux, T.W. Ebbesen, Surface plasmon subwavelength optics, Nature 424 (2003) 824–830.

[4] I. Sondi, B. Salopek-Sondi, Silver nanoparticles as antimicrobial agent: a case study on *E. coli* as a model for Gram negative bacteria, Journal of Colloid and Interface Science 275 (2004) 177–182.

[5] J. Thiel, L. Pakstis, S. Buzby, M. Raffi, C. Ni, D.J. Pochan, S.I. Shah, Antibacterial properties of silver-doped titania, Small 3 (2007) 799–803.

[6] J. Keleher, J. Bashant, N. Heldt, L. Johnson, Y. Li, Photo-catalytic preparation of silver-coated TiO_2 particles for anti-bacterial applications, World Journal of Microbiology and Biotechnology 18 (2002) 133–139.

[7] T. Abe, E. Suzuki, K. Nagoshi, K. Miyashita, M. Kaneko, Electron source in photoinduced hydrogen production on Pt-supported TiO_2 particles, Journal of Physical Chemistry B 103 (1999) 1119–1123.

[8] T. Hirakawa, P.V. Kamat, Charge separation and catalytic activity of Ag@TiO_2 core–shell composites clusters under UV-irradiation, Journal of the American Chemical Society 127 (2005) 1216–1228.

[9] J.M. Herrmann, H. Tahiri, Y. Ait-Ichou, G. Lassaletta, A.R.G. Elipe, A. Fernandez, Characterization and photocatalytic activity in aquous medium of TiO_2 and Ag–TiO_2 coating on quartz, Applied Catalysis B 13 (1997) 219–231.

[10] D.T. Thompson, An overview of gold-catalysed oxidation processes, Topics in Catalysis 38 (2006) 231–240.

[11] M.G. Manera, J. Spadavecchia, D. Buso, C. Julian Fernandez, G. Mattei, A. Martucci, P. Mulvaney, J. Perez-Juste, R. Rella, L. Vasanelli, P. Mazzoldi, Optical gas sensing of TiO_2 and TiO_2/Au nanocomposite thin films, Sensors and Actuators B 132 (2008) 107–115.

[12] R.S. Dhaka, A.K. Shukla, M. Maniraj, S.W. D'Souza, J. Nayak, S.R. Barman, An ultrahigh vacuum compatible sample holder for studying complex metal surfaces, Review of Scientific Instruments 81 (2010) 043907 1-6.

[13] C.C. Chang, J.Y. Chen, T.L. Hsu, C.K. Lin, C.C. Chan, Photocatalytic properties of porous TiO_2/Ag thin films, Thin Solid Films 516 (2008) 1743–1747.

[14] M. Nasr-Esfahani, M.H. Habibi, Silver doped TiO_2 nanostructure composite photocatalyst film synthesized by sol–gel spin and dip coating technique on glass, International Journal of Photoenergy 628713 (2008) 1–11.

[15] Y. Wang, S. Zhang, X. Wu, Synthesis and optical properties of mesostructured titania surfactant inorganic–organic nanocomposites, Nanotechnology 15 (2004) 1162–1165.

[16] V.I. Trofimov, N.M. Sushkova, J. Kim, X-ray photoelectron spectroscopy study of the initial growth of transition metal nanoscale films on (100) Si substrates, Thin Solid Films 515 (2007) 6586–6589.

[17] M. Maeda, T. Yamada, Photocatalytic activity of metal-doped titanium oxide films prepared by sol–gel process, Journal of Physics: Conference Series 61 (2007) 755–759.

[18] K.H. Yang, Y.C. Liu, C.C. Yu, B.C. Chen, New pathway to prepare surface-enhanced Raman scattering-active Au/TiO_2 nanocomposites-containing substrates by sonoelectrochemical methods, Journal of Physical Chemistry C 114 (2010) 12863–12869.

[19] A.R. Malagutti, H.A.J.L. Mourao, J.R. Garbin, C. Ribeiro, Deposition of TiO_2 and Ag:TiO_2 thin films by the polymeric precursor method and their application in the photodegradation of textile dyes, Applied Catalysis B: Environmental 90 (2009) 205–212.

[20] T.G. Schaaff, D.A. Blom, Deposition of Au Nanocrystals on TiO_2 Crystallites, Nano Letters 2 (5) (2002) 507–511.

[21] A.K. Santra, F. Yang, D.W. Goodman, The growth of Ag-Au bimetallic nanoparticles on TiO_2 (110), Surface Science 548 (2004) 324–332.

[22] D.A. Chen, M.C. Bartlet, S.M. Seutter, K.F. McCarty, Small, uniform, and thermally stable silver particles on TiO_2 (110)–(1X1), Surface Science 464 (2000) L708–L714.

[23] C.H. Liu, M.H. Hong, Y. Zhou, G.X. Chen, M.M. Saw, A.T.S. Hor, Synthesis and characterization of Ag deposited TiO_2 particles by laser ablation in water, Physica Scripta T129 (2007) 326–328.

[24] J.C.G. Maxwell, Colours in metal glasses and in metallic films, Philosophical Transactions of the Royal Society of London 203 (1904) 385–420.

[25] A.P. Alivisatos, Perspectives on the physical chemistry of semiconductor nanocrystals, Journal of Physical Chemistry 100 (1996) 13226–13239.

[26] G. Schmid, L.F. Chi, Metal clusters and colloids, Advanced Materials (Weinheim, Germany) 10 (1998) 515–526.

[27] W. Rechberger, A. Hohenau, A. Leitner, J.R. Krenn, B. Lamprecht, F.R. Aussenegg, Optical properties of two interacting gold nanoparticles, Optics Communications 220 (2003) 137–141.

[28] L.M. Liz-Marzan, P. Mulvaney, The assembly of coated nanocrystals, Journal of Physical Chemistry B 107 (2003) 7312–7326.

[29] L.M. Liz-Marzan, M. Giersig, P. Mulvaney, Synthesis of nanosized gold–silica core–shell particles, Langmuir 12 (1996) 4329–4335.

[30] T. Okamoto, In Near Field Optics and Surface Plasmon Polaritons, 2nd ed., Springer, Berlin, 2001.